Syntheses, Structures and Redox Properties of Tetrakis-(μ-benzamidato)-dirhodium(II) Complexes

AKHIL R. CHAKRAVARTY, F. ALBERT COTTON*, DEREK A. TOCHER and JOANNE H. TOCHER

Department of Chemistry and Laboratory for Molecular Structure and Bonding, Texas A&M University, College Station, Tex. 77843, U.S.A.

Received September 28, 1984

Abstract

The reaction of $Rh_2(O_2CCH_3)_4$ with an excess of molten $PhCONH_2$ gave $Rh_2(PhCONH)_4(PhCONH_2)_2$ (**1**) which contains a dirhodium unit having four bridging benzamidato anions and two axial, neutral benzamide ligands. The compound has been characterized by elemental analysis and infrared spectroscopic data. Reactions of (**1**) with $SbPh_3$ and pyridine in CH_2Cl_2 afford crystalline $Rh_2(PhCONH)_4(SbPh_3)_2 \cdot CH_2Cl_2$ (**2**) and $Rh_2(PhCONH)_4(py)_2$ (**3**), respectively. The structures of (**2**) and (**3**) were determined from single-crystal X-ray diffraction data. Compound (**2**) crystallizes in the triclinic space group $P\bar{1}$ with half of the dimer and half of the CH_2Cl_2 molecule constituting the asymmetric unit. The cell dimensions for (**2**) are: a = 12.927(7) Å, b = 13.661(5) Å, c = 10.242(6) Å, α = 103.45(4)°, β = 99.63(4)°, γ = 67.44(4)°, V = 1622(1) Å^3, and Z = 1. The molecule, which has a crystallographic center of inversion, consists of a dirhodium unit bridged by four benzamidato ligands. Each rhodium has one axial ligand, $SbPh_3$. The Rh–Rh distance is 2.463(1) Å and the Rh–Sb bond length is 2.681(1) Å. The mean Rh–O and Rh–N distances are 2.029[4] Å and 2.056[3] Å, respectively. The Rh–Rh–Sb angle is essentially linear having a value of 176.40(2)°. The compound (**3**) crystallizes in the orthorhombic space group *Pbca* with the following unit cell dimensions: a = 16.395(2) Å, b = 18.250(2) Å, c = 11.754(1) Å, $\alpha = \beta = \gamma = 90.0°$, V = 3517(1) Å^3, and Z = 4. Half of the molecule constitutes the asymmetric unit. The molecule has two pyridine ligands in the axial positions. The equatorial positions are occupied by four anionic benzamidato ligands as in (**2**). The Rh–Rh distance is 2.437(1) Å. The distance between the rhodium and the axial pyridine nitrogen atoms is 2.227(7) Å and the angle Rh–Rh–N(3) is 175.5(2)°. The averages of the Rh–O and Rh–N bond lengths are 2.059[6] Å and 2.050[7] Å, respectively. Electron transfer behavior of (**1**) in different solvents and in the presence of strong neutral donor ligands has been investigated. The compound (**1**) in THF, DMF and CH_3CN exhibits a prominent oxidation wave at $E_{1/2}$ = +0.42 V (ΔE_p = 100 mV), +0.23 V (58 mV), and +0.36 V (65 mV), respectively. The pyridine, dithiane, PPh_3 and $SbPh_3$ adducts of (**1**) in CH_2Cl_2 show the first oxidation at +0.39 V (60 mV), +0.48 V (90 mV), +0.46 V (65 mV) and +0.47 V (200 mV), respectively. The PPh_3 adduct displays another quasireversible oxidation at +1.1 V (90 mV). In THF, the pyridine and PPh_3 adducts undergo oxidation at +0.35 V and +0.60 V, respectively. In DMF, the PPh_3 adduct shows oxidation at +0.50 V. In most of the cases, a second, less prominent oxidation wave was observed at slightly higher potential than the prominent oxidation peak. The electronic spectra of the pyridine, PPh_3 and $SbPh_3$ adducts show low energy absorption at 460 nm (shoulder), 445 nm (shoulder), and 508 nm (ϵ = 1520 M^{-1} cm^{-1}), respectively. The electronic spectra of (**1**) studied in several polar solvents display bands in the range 440–563 nm.

Introduction

Widespread current interest [1–25] in the structure and reactivity of dirhodium complexes is due primarily to (i) the ease of preparation and the stability of the complexes, (ii) the ability of the dirhodium unit to undergo axial ligation, (iii) their reversible redox chemistry, (iv) their catalytic [18–20] and biological [21–25] activities. In most of the studies, dirhodium tetracarboxylates have been used. The mono- or diadducts of the Rh_2(carboxylato)$_4$ core have been prepared and characterized by X-ray crystallography with a variety of neutral ligands. Spectroscopic results and theoretical calculations done on these tetracarboxylates show [10,

*Author to whom correspondence should be addressed.

0020-1693/85/$3.30

26–32] the metal–metal bond order to be 1.0 with the ground state configuration $\sigma^2\pi^4\delta^2\delta^{*2}\pi^{*4}$. The Rh–Rh distances lie in the range 2.37–2.49 Å. Crystallographic studies have shown [1] that the Rh–Rh distance is dependent on both the type of bridging carboxylates and the nature of the axial ligands. It is also known that the mode of axial coordination is dependent on the nature of R of the bridging $RCOO^-$. Work from this laboratory has shown [33, 34] that in $Rh_2(O_2CR)_4(Me_2SO)_2$, the axial coordination is through S of the Me_2SO when R = CH_3 or C_2H_5, but it is through oxygen when R = CF_3.

Further illustrations [5, 7, 11–15, 35–38] of the influence of various three-atom bridging ligands on the properties of the Rh_2^{4+} unit are provided by complexes in which these ligands are CO_3^{2-}, SO_4^{2-}, $H_2PO_4^-$, CH_3CSO^-, $R'NC(O)R^-$, dimen (which is 1,8-diisocyanomethane), and the Xhp^- ligands, which are 6-fluoro, 6-chloro or 6-methyl derivatives of 2-oxopyridine.

Bear and coworkers have pioneered the study of $Rh_2(amidato)_4$ compounds [11–15] and in the case of $Rh_2[HNC(O)CF_3]_4py_2$ they have provided an X-ray crystallographic characterization of the molecule. However, we felt that further studies in this area were warranted, with the particular objectives of getting more structural data and more information on the binding of axial ligands. We therefore undertook the preparation of compounds containing the benzamidato anion, $HNC(O)Ph^-$ and we have been successful in preparing and characterizing several compounds containing the $Rh_2(HNC(O)Ph)_4$ moiety.

Electrochemical studies on dirhodium complexes have shown that they typically exhibit reversible electron transfer process(es). Replacement of the carboxylato by the amidato ligands results [11–14] in a cathodic shift of the oxidation potentials (*i.e.*, oxidation becomes more favorable). In some amidato species, a second oxidation of the dirhodium unit is known [11, 14] to occur within the solvent cut-off limit. Recently, Bottomley and Hallberg investigated [17] the electrochemical oxidation of several dirhodium tetracarboxylates and they observed that the oxidation potentials which range from +1.55 V to +1.21 V *vs.* SCE are dependent on the type of R in $RCOO^-$. They also found [17] that for a given carboxylate, the oxidation potential is sensitive to the nature of the axial ligands. Strong σ-donor ligands cause a cathodic shift of the oxidation potential by pushing more electron density to the d_{z^2}(MO) of the rhodium atom. In this paper the details of electrochemical investigations done on the rhodium benzamidato species in various solvents and in presence of several bases will be reported and a comparison made with previously reported data for carboxylato and amidato complexes of dirhodium(II).

Experimental

Materials

Rhodium(II) acetate, $Rh_2(O_2CCH_3)_4(CH_3OH)_2$, was prepared by a literature method [39]. Benzamide, $PhCONH_2$, was purchased from Aldrich Chemical Company.

Preparation of $Rh_2(PhCONH)_4(PhCONH_2)_2$, (1)

A mixture of 0.1 g of $Rh_2(O_2CCH_3)_4(CH_3OH)_2$ and 2 g of benzamide was heated at 140 °C for 48 h under a dinitrogen atmosphere. At this temperature, the ligand was in the molten condition. The excess ligand was removed by sublimation under vacuum at 140 °C. The brown residue was washed several times with dichloromethane and diethylether to remove any trace of unreacted ligand. The yield was quantitative.

Anal. Calcd. for $Rh_2(PhCONH)_4(PhCONH_2)_2$: C, 54.54; H, 4.11; N, 9.09. Found: C, 54.03; H, 3.97; N, 8.64. Infrared spectrum in KBr phase shows bands at: 3360 (s, br), 3180 (s, br), 3040 (w), 1650 (s), 1635 (s), 1595 (s), 1560 (s), 1445 (s), 1425 (s), 1390 (s), 1215 (s), 1115 (s), 1025 (m), 1000 (w), 925 (m), 835 (m), 790 (m), 695 (s), 665 (s), 650 (s), 540 (sh), 520 (m), 465 (w), 415 (w), 440 (w) cm^{-1} (s, strong; m, medium; w, weak; br, broad; sh, shoulder). The compound is sparingly soluble in common non-polar solvents. It is soluble in polar organic solvents like dimethylformamide and dimethylsulfoxide, but only slightly soluble in acetonitrile, acetone and tetrahydrofuran. Attempts to crystallize the product were unsuccessful; only powders were obtained.

Preparation of $Rh_2(PhCONH)_4(L)_2$ (L = py, PPh_3, $SbPh_3$)

The adducts were easily obtained by reacting (**1**) in CH_2Cl_2 with the axial ligand, L. The yield is quantitative. The products were soluble in CH_2Cl_2 though (1) was sparingly soluble in that solvent. In a typical reaction, 50 mg of (**1**) was suspended in 10 mL CH_2Cl_2. To this suspension a slight excess of the stoichiometric amount of L was added. In the case of pyridine or PPh_3, the color of the solution was yellow while for the $SbPh_3$ adduct the color was orange.

The compound $Rh_2(PhCONH)_4(SbPh_3)_2 \cdot CH_2Cl_2$ (**2**) was obtained in crystalline form by slow diffusion of methanol into a CH_2Cl_2 solution of the compound. The solvent of crystallization is very labile and the compound loses crystallinity on removal from the solution. The same is observed for the PPh_3 adduct which was obtained in a similar way. The orange-yellow compound $Rh_2(PhCONH)_4(py)_2$ (**3**) was obtained in crystalline form by slow evaporation of a CH_2Cl_2/hexane mixture. The crystals of

compounds (2), (3) and the PPh_3 adduct are sparingly soluble in CH_2Cl_2, CH_3CN.

Measurements

The elemental analysis of (1) was obtained from Galbraith Lab., Inc. The infrared spectrum was recorded with a Perkin-Elmer 785 spectrophotometer. Electronic spectra were obtained by using a Cary 17D spectrophotometer. Electrochemical measurements were done with a Bioanalytical Systems, Inc. Model BAS 100 Electrochemical Analyser instrument in connection with a Bausch and Lomb, Houston Instruments Model DMP 40 digital plotter. Experiments were done on several solutions containing 0.1 M tetrabutylammonium tetrafluoroborate. In a three-electrode cell system, a platinum disk, Model BAS MF 2032, and a platinum wire were used as working and auxiliary electrodes, and a BAS MF 2020 Ag–AgCl cell was used as reference electrode. All potentials were referenced to the Ag–AgCl electrode at 22 ± 2 °C and are uncorrected for junction potentials. All voltammetric measurements were made under a dry argon atmosphere.

X-ray Crystallographic Procedures

The molecular structures of the single crystals of (2) and (3) were obtained by using the general procedures which are described elsewhere [40–42]†. Detailed descriptions are given below. The crystal parameters and basic information pertaining to data collection and structure refinement are summarized in Table I.

$Rh_2(PhCONH)_4(SbPh_3)_2 \cdot CH_2Cl_2$, (2)

An orange colored crystal of approximate size 0.4 × 0.4 × 0.3 mm was wedged inside a glass capillary containing the mother liquor. Both ends of the capillary was sealed carefully so that the crystal was in the mother liquor. All geometric and intensity data were taken from this crystal by using an automated four-circle diffractometer (Enraf-Nonius CAD-4), equipped with graphite monochromated MoKα radiation. The crystal orientation matrix and unit cell parameters were obtained from a least

†Calculations were done on the VAX-11/780 computer at the Department of Chemistry, Texas A&M University, College Station, Texas with a VAX-SDP software package.

TABLE I. Crystallographic Data for Two $Rh_2(PhCONH)_4(B)_2$ Complexes (B = $SbPh_3$ or Py).

Formula	$Rh_2Sb_2O_4N_4C_{64}H_{54} \cdot CH_2Cl_2$ (2)	$Rh_2O_4N_6C_{38}H_{34}$ (3)
Formula weight	1477.41	844.54
Space group	$P\bar{1}$	*Pbca* (#61)
Systematic absences	None	$h00$: $h = 2n$; $0k0$: $k = 2n$; $00l$: $l = 2n$; $hk0$: $k = 2n$, $h0l$: $h = 2n$; $0kl$: $l = 2n$
a (Å)	12.929(7)	16.395(2)
b (Å)	13.661(5)	18.250(2)
c (Å)	10.242(6)	11.754(1)
α (degrees)	103.45(4)	90.0
β (degrees)	99.63(4)	90.0
γ (degrees)	67.77(4)	90.0
V (Å^3)	1622(1)	3517(1)
Z	1	4
d_{calc} (g/cm^3)	1.516	1.595
Crystal size (mm)	0.4 × 0.4 × 0.3	0.4 × 0.4 × 0.2
μ(Mo Kα) cm^{-1}	14.53	9.71
Data collection instrument	Enraf-Nonius CAD-4	Syntex $P\bar{1}$
Radiation (monochromated in incident beam)	Mo (Kα = 0.71073)	Mo (Kα = 0.71073)
Orientation reflections, number, range (2θ)	25, 16° < 2θ < 38°	15, 20° < 2θ < 30°
Temperature (°C)	25	5
Scan method	ω–2θ	ω–2θ
Data col. range, 2θ (deg.)	5 ⩽ 2θ ⩽ 50	5 ⩽ 2θ ⩽ 50
No. unique data, total with $F_o^2 > 3\sigma(F_o^2)$	5673, 4529	3028, 1728
Number of parameters refined	343	226
Trans. factors, max., min.	99.97%, 86.42%	99.91%, 74.23%
R[a]	0.056	0.062
R_w[b]	0.091	0.077
Quality of fit indicator[c]	2.28	1.60
Largest shift/e.s.d., final cycle	0.17	0.05
Largest peak, e/Å^3	2.2	1.5

[a]$R = \Sigma||F_o| - |F_c||/\Sigma|F_o|$. [b]$R_w = [\Sigma w(|F_o| - |F_c|)^2/\Sigma w|F_o|^2]^{1/2}$; $w = 1/\sigma^2(|F_o|)$. [c]Quality of fit = $[\Sigma w(|F_o| - |F_c|)^2/(N_{obs} - N_{parameters})]^{1/2}$.

squares fit to the goniometer settings of 25 accurately located reflections in the range $16° < 2\theta < 38°$. Data scans, which employed an ω–2θ motion, were made for 5673 reflections in the range $5° \leqslant 2\theta \leqslant 50°$. Data were collected at a fast rate and there was decay of 31% during only 43.2 hours exposure time. A decay correction was applied. In the absence of mother liquor, the crystals lost their crystallinity spontaneously. An empirical absorption correction was made (μ(MoKα) = 14.534 cm^{-1}) based on azimuthal scans of 9 reflections with Eulerian angle χ near 90°.

From unit cell dimensions and axial photographs, the crystals were found to be triclinic. There were no systematic absences. The positions of the heavy atoms Sb and Rh were found by the direct methods program MULTAN. The remainder of the structure was located and refined, assuming the space group to be $P\bar{1}$, by an alternating sequence of least-squares cycles and difference Fourier maps. At the end of the refinement, a CH_2Cl_2 molecule was found in the difference Fourier map. The C and Cl atoms of the CH_2Cl_2 were refined with a site occupancy factor of 0.5. The asymmetric unit thus has one half of the complex molecule and half of the solvent molecule. The solvent molecule does not interact with the complex molecule and is present as a solvent of crystallization. Since the isotropic thermal parameters of the CH_2Cl_2 molecule were high, it was refined isotropically. In the last cycle of least-squares refinement, these atoms were kept in the structure factor calculation but not refined. In the final difference Fourier map three peaks with values of 2.2, 1.7 and 1.7 e/Å^3 were found near the CH_2Cl_2 molecule. The positional parameters (x, y, z) of these three peaks, peaks 1–3, are respectively 0.6660, 0.3535, 0.3047; 0.1445, 0.5410, 0.5273; 0.7285, 0.4570, 0.4434. The distances and angles are peak 1–peak 3 = 2.053 Å; peak 2–peak 3 = 1.622 Å, and peak 1–peak 3–peak 2 = 130°. Peak 1 is 1.42 Å from Cl(2), peak 2 is 0.69 Å from Cl(1), and peak 3 is 1.44 Å from C(1). The CH_2Cl_2 molecule refined in the least-square cycles is thus disordered. We did not add these three peaks near the CH_2Cl_2 molecule because they are weak and without the addition of these peaks whole molecule refined well. The final cycle which changed no parameter by more than 0.17 times its estimated standard deviation, involved 4529 data and 343 parameters. The final R-factors (summarized and defined in Table I) are R = 0.056 and R_w = 0.091, with a quality-of-fit indicator of 2.28.

$Rh_2(PhCONH)_4(py)_2$, (3)

A yellow single crystal of approximate size 0.4 × 0.4 × 0.2 mm was mounted on a glass fiber. All geometric and intensity data were collected on a Syntex $P\bar{1}$ diffractometer using Mo-Kα radiation with a graphite crystal monochromator in the incident beam. The lattice vectors were obtained using the automatic indexing routine of the diffractometer with the 15 reflections taken from a rotation photograph and located and centered by the diffractometer. Axial photography was used to verify the unit cell dimensions. Precise cell dimensions along with the crystal orientation matrix were obtained from a least-squares fit of 15 strong reflections in the range $20° < 2\theta < 30°$. Data were collected at 5 °C with use of the ω–2θ scan technique in the range $5° \leqslant 2\theta \leqslant 50°$. There was no significant change in intensity during 110.6 hours of exposure time. Corrections were made for Lorentz and polarization effects. The crystals belong to the orthorhombic crystal system and the space group was found to be Pbca from the systematic absences.

The position of the Rh atom was obtained by solving the three dimensional Patterson map and the remaining structure was obtained from successive iterations, difference Fourier maps and least squares cycles. The problem of choosing the positions for N and O in the benzamide ligand was handled by monitoring the isotropic thermal parameters of the N and O atoms. For example, in (3), interchanging the positions of O(2) and N(2) gave isotropic thermal parameters as 5.005 and 1.864, indicating that the first assignments were preferable. However, the change was not significant in the case of O(1) and N(1) atoms, and thus the arrangement there remains ambiguous.

In the final cycle of refinement all the atoms were refined anisotropically. The final cycle gave the residuals R = 0.062 and R_w = 0.077, with quality-of-fit 1.5. The final difference Fourier map was featureless.

Results

Syntheses

The reaction of $Rh_2(O_2CCH_3)_4$ with molten benzamide took place smoothly to give a quantitative yield of brown $Rh_2(PhCONH)_4(PhCONH_2)_2$, (1), which was characterized by elemental and infrared spectroscopic studies. It is sparingly soluble in common organic solvents, slightly soluble in acetonitrile, tetrahydrofuran, and soluble in dimethylformamide and dimethyl sulfoxide. The infrared spectrum shows characteristic absorption bands of benzamide. The presence of the N–H and carbonyl parts of the amide functionality is evidenced from the bands at 3360, 3180 cm^{-1} and 1650, 1635 cm^{-1}, respectively. Addition of bases, L, like pyridine, $SbPh_3$ and PPh_3 gave dirhodium compounds $Rh_2(PhCONH)_4(L)_2$ with four bridging benzamide ligands and two axial ligands. The pyridine and $SbPh_3$ adducts were characterized by X-ray crystallography.

Molecular Structures

The positional and thermal parameters of $Rh_2(PhCONH)_4(SbPh_3)_2 \cdot CH_2Cl_2$ (2) and $Rh_2(PhCONH)_4(py)_2$ (3) are presented in Tables II and III, respectively. Selected bond lengths and angles of the compounds (2) and (3) are listed in Tables IV and V, respectively.

Compound (2) crystallizes in the triclinic space group $P\bar{1}$. The ORTEP diagram of the dimeric molecule along with the atom numbering scheme is shown in Fig. 1. There is a crystallographic center of inversion in the molecule. The Rh(1)–Rh(1)′ bond length is 2.463(1) Å. Each rhodium atom is in an essentially octahedral environment with a $Rh'SbO_2N_2$ coordination sphere. The arrangement of bridging ligands is of the 2:2 type. The Rh(1)–Sb(1) distance is 2.681(1) Å. The mean Rh–O and Rh–N bond lengths are 2.029[4] Å and 2.056[3] Å, respectively. The average Sb–C distance is 2.122[5] Å. The mean O–C and N–C distances are 1.304[4] Å and 1.281-[6] Å, respectively. The Sb(1)–Rh(1)–Rh(1)′ chain is essentially linear having the angle 176.40(2)°. The average Sb(1)–Rh(1)–O and Sb(1)–Rh(1)–N angles are 93.1[1] and 92.14[9]°, respectively. While the Sb(1)–Rh(1)–O and Sb(1)–Rh(1)–N angles are all obtuse, the Rh(1)′–Rh(1)–O and Rh(1)′–Rh(1)–N angles are all acute, being respectively 85.5[1]° and 89.29[10]°. The O(1)–Rh(1)–O(2) and N(1)–Rh(1)–N(2) angles are 91.9-(2)° and 90.1(2)°, respectively. The lattice CH_2Cl_2 molecule, which does not interact with the complex molecule, has an average C–Cl bond length of 1.811 Å and the Cl(1)–C(1)–Cl(2) angle is 125.13°. The CH_2Cl_2 molecule is disordered as mentioned in the experimental section.

TABLE II. Table of Positional Parameters and Their e.s.d.s for $Rh_2(PhCONH)_4(SbPh_3)_2 \cdot CH_2Cl_2$[a].

Atom	*x*	*y*	*z*	*B*(*A*2)
Sb1	0.25031(3)	0.02587(3)	0.76090(4)	3.134(9)
Rh1	0.07623(3)	0.01214(3)	0.58409(4)	2.73(1)
O1	0.1001(5)	0.0983(4)	0.4602(5)	4.8(1)
O2	0.1735(4)	−0.1281(4)	0.4804(5)	4.7(1)
N1	−0.0385(4)	0.0733(4)	0.3026(5)	2.9(1)
N2	0.0362(4)	−0.1534(4)	0.3197(5)	2.7(1)
C11	0.0401(5)	0.1115(5)	0.3479(6)	3.4(1)
C12	0.0545(6)	0.1820(6)	0.2625(7)	4.2(2)
C13	0.0892(7)	0.2692(6)	0.3196(9)	6.2(2)
C14	0.1039(9)	0.3293(8)	0.238(1)	7.7(3)
C15	0.0745(9)	0.3085(8)	0.099(1)	7.5(3)
C16	0.0375(8)	0.2242(7)	0.0419(9)	6.0(2)
C17	0.0256(6)	0.1620(6)	0.1252(7)	5.0(2)
C21	0.1378(5)	−0.1846(5)	0.3723(6)	3.1(1)
C22	0.2178(6)	−0.2905(5)	0.3035(7)	3.8(2)
C23	0.1734(8)	−0.3623(6)	0.2170(8)	5.2(2)
C24	0.245(1)	−0.4570(8)	0.154(1)	7.0(3)
C25	0.362(1)	−0.4874(8)	0.179(1)	7.3(3)
C26	0.4034(8)	−0.4151(8)	0.265(1)	7.0(3)
C27	0.3329(7)	−0.3162(7)	0.3293(9)	5.4(2)
C41	0.2860(6)	0.1693(6)	0.7976(7)	4.0(2)
C42	0.3911(6)	0.1746(7)	0.3497(8)	5.5(2)
C43	0.4112(8)	0.2712(6)	0.8676(9)	6.0(2)
C44	0.3304(9)	0.3580(7)	0.835(1)	8.3(3)
C45	0.224(1)	0.3569(7)	0.784(1)	7.7(3)
C46	0.2027(8)	0.2599(6)	0.7641(9)	5.6(2)
C51	0.2738(6)	−0.0130(5)	0.9551(6)	3.6(2)
C52	0.2348(7)	−0.0921(6)	0.9675(8)	5.6(2)
C53	0.2418(8)	−0.1176(7)	1.0906(9)	6.1(2)
C54	0.2856(7)	−0.0653(7)	1.2043(8)	5.5(2)
C55	0.3226(7)	0.0136(8)	1.1928(8)	5.3(2)
C56	0.3183(6)	0.0408(6)	1.0693(7)	4.1(2)
C61	0.4037(6)	−0.0872(5)	0.6853(7)	3.8(2)
C62	0.4303(6)	−0.0779(6)	0.5593(7)	4.5(2)
C63	0.5230(8)	−0.1560(8)	0.5013(9)	6.1(2)
C64	0.5906(8)	−0.2390(8)	0.558(1)	7.1(3)
C65	0.433(1)	0.2467(8)	0.321(1)	8.1(3)
C66	0.4738(7)	−0.1718(7)	0.745(1)	5.8(2)
Cl1	0.8010(9)	0.4596(8)	0.458(1)	13.2(3)*
Cl2	0.6886(9)	0.3642(8)	0.179(1)	12.6(3)*
C1	0.756(2)	0.357(2)	0.349(3)	12.4(7)*

[a]Starred atoms were refined isotropically. Anisotropically refined atoms are given in the form of the isotropic equivalent thermal parameter defined as $4/3[a^2\beta_{11} + b^2\beta_{22} + c^2\beta_{33} + ab(\cos\gamma)\beta_{12} + ac(\cos\beta)\beta_{13} + bc(\cos\alpha)\beta_{23}]$.

TABLE III. Table of Positional Parameters and Their e.s.d.s for $Rh_2(PhCONH)_4(py)_2$ (3)[a].

Atom	*x*	*y*	*z*	*B*(*A*2)
Rh1	−0.02204(5)	−0.04235(7)	−0.05764(4)	2.87(1)
O1	0.0326(5)	−0.1894(7)	−0.0223(4)	4.7(2)
O2	0.0853(4)	0.0113(6)	−0.1059(4)	3.4(1)
N1	−0.0737(5)	0.1119(6)	−0.0870(4)	2.7(2)
N2	−0.1253(5)	−0.0868(7)	−0.0036(5)	3.3(2)
N3	−0.0520(5)	−0.1211(8)	−0.1653(5)	3.9(2)
C1	−0.0822(7)	−0.227(1)	−0.1727(7)	5.0(3)
C2	−0.0891(8)	−0.280(1)	−0.2399(8)	6.8(4)
C3	−0.0591(9)	−0.226(1)	−0.3021(7)	6.8(4)
C4	−0.0280(8)	−0.114(1)	−0.2966(6)	6.0(3)
C5	−0.0261(7)	−0.069(1)	−0.2257(6)	4.4(3)
C11	−0.0696(6)	0.193(1)	−0.0416(6)	3.7(2)
C12	−0.1118(6)	0.3035(9)	−0.0603(6)	3.6(2)
C13	−0.1675(7)	0.303(1)	−0.1194(7)	4.7(3)
C14	−0.2095(8)	0.404(1)	−0.1392(9)	6.4(4)
C15	−0.1936(9)	0.502(1)	−0.1008(9)	7.1(4)
C16	−0.1369(9)	0.504(1)	−0.0431(9)	6.6(4)
C17	−0.0959(8)	0.403(1)	−0.0215(7)	5.0(3)
C21	−0.1360(6)	−0.0662(7)	0.0663(5)	2.8(2)
C22	−0.2104(6)	−0.1115(9)	0.1050(6)	3.4(2)
C23	−0.2456(7)	−0.217(1)	0.0838(6)	4.3(2)
C24	−0.3131(8)	−0.256(1)	0.1239(8)	5.9(3)
C25	−0.3423(8)	−0.199(1)	0.1866(7)	6.5(4)
C26	0.3056(8)	0.096(1)	−0.2062(8)	6.0(3)
C27	−0.2386(7)	−0.051(1)	0.1664(6)	4.7(3)

[a]Anisotropically refined atoms are given in the form of the isotropic equivalent thermal parameter defined as $4/3[a^2\beta_{11} + b^2\beta_{22} + c^2\beta_{33} + ab(\cos\gamma)\beta_{12} + ac(\cos\beta)\beta_{13} + bc(\cos\alpha)\beta_{23}]$.

TABLE IV. Selected Bond Distances and Angles for $Rh_2(PhCONH)_4(SbPh_3)_2 \cdot CH_2Cl_2$ (2)[a].

Bond distances (Å)			
Rh(1)–Rh(1)′	2.463(1)	O(1)–C(11)	1.288(6)
Rh(1)–Sb(1)	2.681(1)	O(2)–C(21)	1.319(6)
Rh(1)–O(1)	2.045(4)	N(1)–C(11)	1.281(6)
Rh(1)–O(2)	2.012(4)	N(2)–C(21)	1.281(6)
Rh(1)–N(1)	2.046(3)	C(11)–C(12)	1.581(7)
Rh(1)–N(2)	2.065(3)	C(21)–C(22)	1.513(7)
Sb(1)–C(41)	2.110(5)	C(1)–Cl(1)	1.794
Sb(1)–C(51)	2.126(4)	C(1)–Cl(2)	1.827
Sb(1)–C61)	2.129(5)		
Bond angles (deg.)			
Sb(1)–Rh(1)–Rh(1)′	176.40(2)	O(1)–Rh(1)–O(2)	91.9(2)
Sb(1)–Rh(1)–O(1)	94.7(1)	O(1)–Rh(1)–N(1)	174.6(2)
Sb(1)–Rh(1)–O(2)	91.5(1)	O(1)–Rh(1)–N(2)	88.8(2)
Sb(1)–Rh(1)–N(1)	90.6(1)	O(2)–Rh(1)–N(1)	88.8(2)
Sb(1)–Rh(1)–N(2)	93.67(9)	O(2)–Rh(1)–N(2)	174.8(1)
Rh(1)′–Rh(1)–O(1)	86.0(1)	N(1)–Rh(1)–N(2)	90.1(2)
Rh(1)′–Rh(1)–O(2)	85.0(1)	O(1)–C(11)–N(1)	124.7(4)
Rh(1)′–Rh(1)–N(1)	88.7(1)	O(2)–C(21)–N(2)	122.8(4)
Rh(1)′–Rh(1)–N(2)	89.87(9)	Cl(1)–C(1)–Cl(2)	125.13
Rh(1)–Sb(1)–C(41)	117.9(2)		
Rh(1)–Sb(1)–C(51)	122.9(1)		
Rh(1)–Sb(1)–C(61)	110.0(1)		
C(41)–Sb(1)–C(51)	103.4(2)		
C(41)–Sb(1)–C(61)	100.1(2)		
C(51)–Sb(1)–C(61)	98.8(2)		

[a]Numbers in parentheses are e.s.d.s in the least significant digits.

TABLE V. Selected Bond Distances and Angles for $Rh_2(PhCONH)_4(py)_2$ (3)[a].

Bond distances (Å)			
Rh(1)–Rh(1)′	2.437(1)	O(2)–C(21)	1.277(9)
Rh(1)–O(1)	2.050(6)	N(2)–C(21)	1.311(10)
Rh(1)–O(2)	2.067(6)	C(21)–C(22)	1.505(11)
Rh(1)–N(1)	2.072(6)		
Rh(1)–N(2)	2.028(7)		
Rh(1)–N(3)	2.227(7)		
O(1)–C(11)	1.315(10)		
N(1)–C(11)	1.267(11)		
C(11)–C(12)	1.508(12)		
Bond angles (deg.)			
Rh(1)′–Rh(1)–O(1)	86.7(2)	O(2)–Rh(1)–N(2)	175.5(3)
Rh(1)′–Rh(1)–O(2)	89.5(2)	O(2)–Rh(1)–N(3)	86.5(3)
Rh(1)′–Rh(1)–N(1)	89.2(2)	N(1)–Rh(1)–N(2)	90.5(3)
Rh(1)′–Rh(1)–N(2)	86.2(2)	N(1)–Rh(1)–N(3)	92.6(3)
Rh(1)′–Rh(1)–N(3)	175.5(2)	N(2)–Rh(1)–N(3)	97.9(3)
O(1)–Rh(1)–O(2)	91.1(3)	O(1)–C(11)–N(1)	125.3(9)
O(1)–Rh(1)–N(1)	176.0(3)	O(2)–C(21)–N(2)	123.8(7)
O(1)–Rh(1)–N(2)	89.7(3)		
O(1)–Rh(1)–N(3)	91.4(3)		
O(2)–Rh(1)–N(1)	88.3(3)		

[a]Numbers in parentheses are e.s.d.s in the least significant digits.

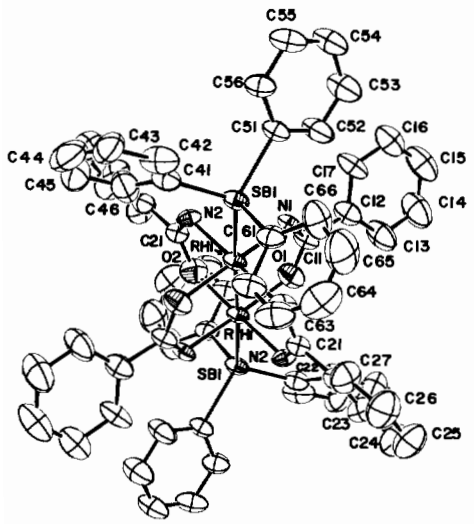

Fig. 1. An ORTEP diagram at 50% probability level of $Rh_2(PhCONH)_4(SbPh_3)_2$ along with atom labelling scheme.

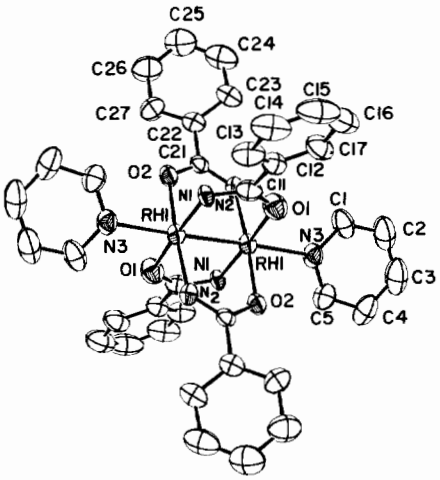

Fig. 2. An ORTEP diagram of $Rh_2(PhCONH)_4(py)_2$ along with atom labelling scheme. Atoms are represented by thermal ellipsoid at 50% probability level.

An ORTEP diagram of the $Rh_2(PhCONH)_4(py)_2$ (**3**) molecule along with the atom labeling scheme is shown in Fig. 2. The compound crystallizes in the orthorhombic space group *Pbca*. The molecule consists of four bridging benzamidato and two axial pyridine ligands enclosing an Rh_2^{4+} core. The arrangement of bridging ligands is of the 2:2 type. The Rh–Rh distance is 2.437(1) Å. The axial ligand distance, Rh(1)–N(3), is 2.227(7) Å. The average Rh–O and Rh–N bond lengths in the '$Rh_2(PhCONH)_4$' core are 2.059[6] Å and 2.050[7] Å, respectively. The Rh(1)′–Rh(1)–N(3) angle is 175.5(2)°. The other Rh(1)′–Rh(1)–N and Rh(1)′–Rh(1)–O angles are acute, ranging from 86.2(2)° to 89.5(2)°.

Electrochemistry

Electrochemical results are summarized in Table VI. The compound (**1**), $Rh_2(PhCONH)_4(PhCONH_2)_2$,

TABLE VI. Electrochemical Data for $Rh_2(PhCONH)_4(PhCONH_2)_2$[a].

Solvent	Base	Scan rate ($mV\ s^{-1}$)	$E_{1/2}$ (V *vs.* Ag/AgCl (ΔE_p, mV))
CH_2Cl_2	C_5H_5N	100–500	+0.39 (60), +0.57 (60)
	PPh_3	100	+0.46 (65), +1.1 (90)
	PPh_3	1000	+0.46 (75), +1.1 (100), +1.44[b], +1.68[b]
	$SbPh_3$	50	+0.47 (200)
	p-dithiane[c]	100	+0.48 (90)
C_4H_8O	–	100–500	+0.42 (100), +0.63 (60)
	C_5H_5N	50–500	+0.35 (60), +0.55 (60)
	PPh_3	50–100	+0.60 (65), +1.08 (80)
	PPh_3	500	+0.60 (80), +1.08 (100)
	p-dithiane	100	+0.50 (60), +0.69 (60)
	p-dithiane	500	+0.51 (80), +0.70 (70)
	p-dithiane	1000	+0.51 (100), +0.70 (70)
$HCONMe_2$	–	50	+0.23 (58), +0.44 (60)
	–	500	+0.24 (65), +0.44 (65)
	C_5H_5N	100–500	+0.25 (65), +0.45 (60)
	PPh_3	100	+0.50 (60), +0.92 (60)
	PPh_3	500	+0.50 (70), +0.92 (70)
CH_3CN	–	100	+0.36 (65), +0.59 (60)
	–	500	+0.36 (70), +0.58 (60)

[a]Tetraethylammonium tetrafluoroborate, (TEA)(BF_4), of 0.1 *M* concentration was used as a supporting electrolyte. [b]Anodic peak potential of the irreversible process. [c]*p*-dithiane is $\overline{CH_2-CH_2-S-CH_2-CH_2-S}$.

is insoluble in CH_2Cl_2. Addition of two molar equivalents of pyridine to the suspension of (1) in CH_2Cl_2 readily gives a yellow solution. Cyclic voltammetry of this solution exhibits two oxidation processes at 0.39 V and 0.57 V at scan rates 100 to 500 mVs^{-1}. The electrontransfer process is reversible with the peak-to-peak separation, $\Delta E_p = E_{pa} - E_{pc}$ (E_{pa} and E_{pc} are anodic and cathodic peak potentials, respectively), of 60 mV. The couple at +0.39 V is more prominent. At all scan rates, the ratio of anodic to cathodic peak currents, i_{pa}/i_{pc}, is unity within experimental error. By differential pulse voltammetry a single peak is observed with a peak potential of +0.38 V. The cyclic voltammogram is shown in Fig. 3(a).

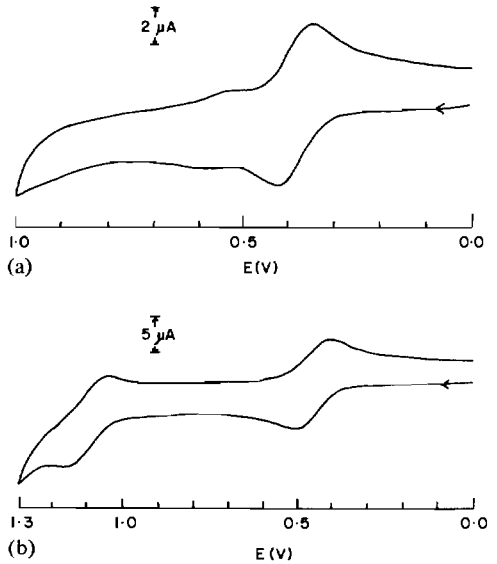

Fig. 3. Cyclic voltammograms of $Rh_2(PhCONH)_4(PhCONH_2)_2$ in CH_2Cl_2 in presence of (a) pyridine and (b) PPh_3.

Addition of PPh_3 to a suspension of (1) in CH_2Cl_2 gives a yellow solution. By cyclic voltammetry we see up to four oxidation processes. While the two at less positive potentials, at +0.46 V and +1.1 V, approach reversibility, the two processes at more positive potentials are irreversible and have a greater current response than the former (*ca.* 2–3 times greater). It is found that inclusion of these processes in the potential scan destroys the reversible character of the wave at +1.1 V, but the first one remains apparently unaffected. Fig. 3(b) shows the cyclic voltammograms of the reversible processes. The ΔE_p value increases on increasing scan rates. The two irreversible processes at more positive potentials have forward wave peak potentials of +1.44 V and +1.68 V. Differential pulse voltammetry shows two well resolved peaks of the same peak currents which correspond to the reversible processes seen in the cyclic voltammetry. The irreversible processes towards more positive potentials are represented by a broad, very ill-defined band. Peak potentials of E_p = +0.44 V and+1.09 V with widths at half height of 95 mV and 100 mV, respectively, are observed although the second oxidation is partially distorted by further oxidations.

Electrochemistry of the solution obtained by adding $SbPh_3$ to the suspension of (1) in CH_2Cl_2 is very indistinct. In the differential pulse, a peak at +0.4 V is present but there is a strong shoulder to more positive potentials making analysis difficult. Cyclic voltammetry of the solution, however, shows a quasireversible oxidation at +0.47 V at 50 mVs^{-1} with a ΔE_p value of 200 mV.

Upon addition of *p*-dithiane, the $Rh_2(PhCONH)_4(PhCONH_2)_2$ complex does not appear to dissolve. However, on close examination it can be seen that the original brown color of the complex (1) has changed to pink, suggesting that a reaction has indeed taken place, but that the product itself is also sparingly soluble in CH_2Cl_2. The cyclic voltammetry of this solution shows a reversible oxidation with $E_{1/2}$ = +0.48 V and ΔE_p = 90 mV at v = 100 mVs^{-1} (v = scan rate). Differential pulse voltammetry of this solution exhibits a single peak with a peak potential E_p = +0.5 V. Owing to the very slight solubility, no further analysis was possible in this solvent.

Compound (1) is soluble enough in tetrahydrofuran (THF) for cyclic voltammetric and differential pulse voltammetric studies. The solution exhibits two closely spaced oxidative processes at +0.42 V and +0.63 V (Fig. 4(a)). The one at less positive potential is by far the more prominent one. There appears to be a shoulder on the return wave of the cyclic voltammograms at +0.42 V at *ca.* E_p + 0.2 V. The differential pulse voltammetry shows two closely resolved peaks with peak potentials of +0.41 V and +0.62 V, the former being by far the more prominent (i_p = 0.59 μA and i_p = 0.14 μA, respectively). The +0. 41 V process shows a definite shoulder at *ca.* +0.225 V (≈same current as +0.62 V process), resulting in +0.41 V being slightly asymmetric in appearance.

Cyclic voltammetry of the solution obtained by adding pyridine to the THF solution of (1) shows two closely spaced oxidative processes at +0.35 V and +0.55 V. Both processes appear to have a high degree of reversibility. The forward-to-return peak current ratio is 1.0 at different scan rates. The process at +0.55 V is clearly present in each scan but could not be studied because of insufficient resolution. Differential pulse voltammetry shows two peaks within the available solvent limit, with peak potentials of E_p = +0.33 V and +0.54 V. The former is more prominent, having peak current of 0.95 μA against 0.013 μA of the latter. The former has a width at half height of 90 mV.

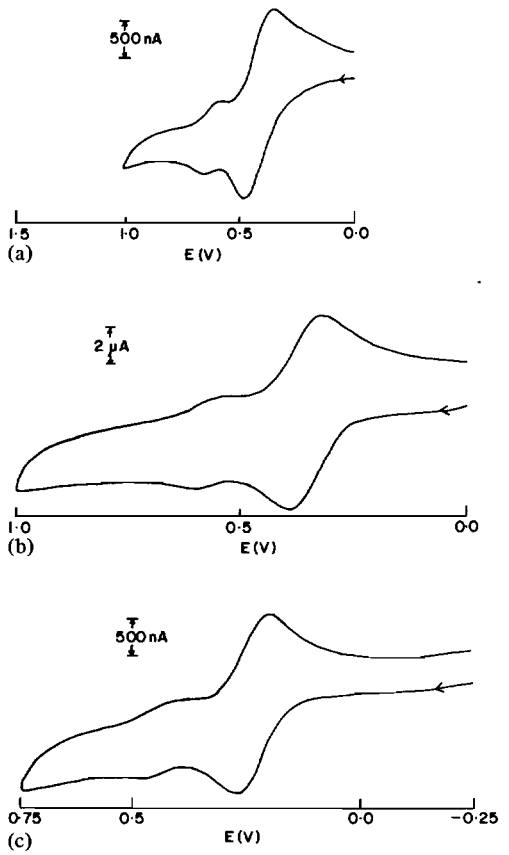

Fig. 4. Cyclic voltammograms of $Rh_2(PhCONH)_4(PhCONH_2)_2$ in (a) tetrahydrofuran, (b) dimethylformamide, and (c) acetonitrile.

Upon addition of PPh_3 into the THF solution of (**1**) we see only two oxidations at +0.60 V and +1.08 V within the more limited positive solvent range for THF. The first response is again highly reversible in nature, while the second shows a clear return wave only at scan rates in the order of 2000 mVs^{-1} suggesting a fast, irreversible following reaction, perhaps due to the close proximity of the solvent front. The first oxidation is not apparently affected by the following reaction of the second oxidation, and its forward-to-return current ratio is 1.0 irrespective of scan rate or switching potential. The differential pulse voltammetry shows quite clearly two oxidation processes with peak potentials of +0.58 V and +1.08 V both having the same peak currents, with width at half-height of 100 mV.

When *p*-dithiane was added to the THF solution of (**1**) an immediate color change was observed and no material was found to be precipitated from the solution. Cyclic voltammetry of the solution shows two oxidations at +0.50 V and +0.69 V, the one to less positive potentials being the more prominent, with a shoulder present on the return wave. The ΔE_p values at slow scan rates are *ca.* 60 mV indicating a reversible electron transfer process but an increase in scan rate increases the ΔE_p values. The differential pulse voltammetry shows two peaks, with peak potentials of E_p = +0.50 V and +0.68 V. The peak current of the first oxidation process is *ca.* 4–5 times greater than that of the second oxidation process.

In dimethylformamide (DMF), the compound (**1**) is readily soluble. Cyclic voltammetry of the DMF solution exhibits two closely spaced oxidations, as shown in Fig. 4(b). The response at +0.23 V (ΔE_p = 58 mV) is more prominent than the response at +0.44 V (ΔE_p = 60 mV). This time no shoulder was found on the main oxidation return wave. Differential pulse voltammetry shows two oxidation processes with peak potentials of E_p = +0.23 V and +0.44 V with peak currents of 1.18 μA and 0.18 μA, respectively. The +0.23 V peak is symmetrical with a 90 mV peak width at half height.

The potentials of the responses remain almost unchanged on addition of pyridine to the DMF solution of (**1**), but an immediate color change was observed upon pyridine addition from orange-brown to bright yellow. Addition of PPh_3 into a DMF solution of (**1**) causes an anodic shift of the peak potentials. The response at +0.50 V (ΔE_p = 60–70 mV) is clearly resolved, the second one at +0.92 V (ΔE_p = 60–70 mV) is greatly obscured by the close proximity of the solvent front. The differential pulse voltammetry, having a slightly wider potential range than the CV shows the two oxidation peaks quite distinctly with peak potential of E_p = +0.48 V and +0.92 V with approximately the same peak current. The former process has a 100 mV peak-width at half-height. The second oxidation is partially obscured by the solvent front at more positive potentials, thus preventing the measurement of the width at half-height.

It is found that acetonitrile has sufficient coordinating ability to dissolve the compound (**1**) and cyclic voltammetry of the acetonitrile solution shows two oxidations at +0.36 V and +0.59 V (Fig. 4c). The ΔE_p values range from 60–70 mV at scan rates v = 50–500 mVs^{-1}. The former process is more prominent than the latter one. At all scan rates the i_{pa}/i_{pc} ratio was found to be unity. Using differential pulse voltammetry, three oxidations are observed with peak potentials of E_p = +0.35 V, +0.57 V, and +1.07 V. The second oxidation corresponds to the process identified by cyclic voltammetry, the first oxidation being much more prominent with a forward wave current of 1.42 μA against 0.32 μA of the second oxidation wave. The oxidation at +0.35 V has a width at half-height of 120 mV. The third oxidation, absent or not resolved by cyclic voltammetry, has approximately the same current response but is slightly less well resolved than the process at +0.57 V.

Electronic Spectra

Spectral data are listed in Table VII. The compound (**1**) is slightly soluble in acetonitrile. The electronic spectrum of the very dilute solution exhibits a band at 488 nm and a shoulder at 340 nm. Compound (**1**) when treated with acetone forms a green solid which appears to be slightly soluble. The solution shows a band at 550 nm with a shoulder at 460 nm. In other polar solvents, the electronic spectrum of (**1**) displays a shoulder at 440 nm in Me_2SO, a band at 563 nm in THF, and a band at 548 nm in DMF.

The electronic spectra of (**1**) in CH_2Cl_2, in presence of bases like pyridine, PPh_3 and $SbPh_3$, have been studied. The pyridine adduct exhibits two shoulders at 460 nm and 340 nm while the $SbPh_3$ adduct shows three bands at 508 nm, 372 nm, and 325 nm. The PPh_3 adduct displays a low-energy shoulder and a band at 380 nm.

Discussion

Compound (**1**) $Rh_2(PhCONH)_4(PhCONH_2)_2$, which has not been crystallized, has been characterized by elemental analysis and infrared spectroscopy. Since (**2**) and (**3**) were obtained as $SbPh_3$ and pyridine adducts from (**1**) it is most likely that the core structure, $Rh_2(PhCONH)_4$, is the same in all three compounds. In (**1**) the axial coordinating ligands are two neutral benzamide ($PhCONH_2$) molecules. This is the first case where such axial ligation has been found; the acetamide [14] and trifluoroacetamide [12] compounds do not have additional amide molecules in the axial positions. Infrared data for (**1**) are consistent with the presence of the axial ligands. The bridging amidato ligands give rise to bands at 1635, 1650, 3180 and 3360 cm^{-1}, the latter being very strong and broad. The first two can be assigned to stretches in the O–C–N chains and the latter to N–H stretches. Comparison can be made to the spectrum of $Os_2Cl_2(PhCONH)_4$ [43] which has bands at 1500, 1595, 3190 and 3318 cm^{-1}. In (**1**) we find two bands in the 1600–1650 cm^{-1} range that are not due to the bridging amidato ligands but can be assigned to the axial benzamide molecules. No bands in this range are found in complexes with bridging benzamidato ligands but lacking axial benzamide molecules [43, 44]. Whether the axial ligands are coordinated through oxygen or nitrogen is unknown.

The presence of (**1**) of both bridging anions and axial neutral molecules is comparable to the situation previously found in $Rh_2(OSCCH_3)_4(CH_3C(S)OH)_2$ [37], where the axial molecules coordinate through the sulfur atoms and there are O–H···O hydrogen bonds from the OH groups of the axial molecules to the oxygen atoms of the bridging ligands.

The most obvious comparison that can be made between the structural work done here and previous work is between the structure of (**3**) and that of $Rh_2(CF_3CONH)_4(py)_2$ [12]. The data are shown in Table VIII along with those for a few other representative compounds. For the trifluoroacetamide compound both the Rh–Rh and the Rh–N bonds are longer, by 0.035 Å and 0.03 Å, respectively. The shorter Rh–Rh distance in the $Rh_2(PhCONH)_4(py)_2$ compound might be attributed to the greater basicity of the bridging ligands, which could make the Rh–Rh core less positive and thus increase the metal–metal overlaps. However, this would also imply that the Rh_2 unit would be less electrophilic and thus form longer rather than shorter bonds to the axial pyridine molecules, contrary to what is found. Evidently this simple sort of argument omits some significant factor. Indeed it is generally not possible, so far as we can see, to account for the small (but real) variations in bond lengths that can be seen in Table VIII by any simple electronic arguments. It is likely that steric factors play a significant role. One steric factor is the smaller bite of RCO_2^- compared to $RCONH^-$, and it does seem that, other things being equal, carboxylato

TABLE VII. Electronic Spectral Data.

Compound	Solvent	λ_{nm} (ϵ, M^{-1} cm^{-1})[a]
$Rh_2(PhCONH)_4(PhCONH_2)_2$	CH_3CN[b]	488, 340 (sh)
	CH_3COCH_3[c]	550, 460 (sh)
	C_4H_8O	563 (170), 340 (sh)
	$(CH_3)_2SO$	440 (sh)
	$HCONMe_2$	548 (250), 350 (sh)
$Rh_2(PhCONH)_4(py)_2$	CH_2Cl_2	460 (sh), 340 (sh)
$Rh_2(PhCONH)_4(PPh_3)_2$	CH_2Cl_2	445 (sh), 380 (18800)
$Rh_2(PhCONH)_4(SbPh_3)_2$	CH_2Cl_2	508 (1520), 372 (30000), 325 (30370)

[a]sh, shoulder. [b]Compound is slightly soluble. [c]The acetone adduct which is yellow green in color is slightly soluble.

TABLE VIII. Comparison of Rh–Rh and Rh–Axial Ligand (L) Bond Lengths in Some Selected Dirhodium Compounds.

Compound	Rh–Rh (Å)	Rh–L (Å)	Ref.
$Rh_2(O_2CCH_3)_4(H_2O)_2$	2.3855(5)	2.310(3)	46
$Rh_2(O_2CC_2H_5)_4(aza)_2$[a]	2.403(1)	2.266(6), 2.284(6)	4
$Rh_2(O_2CCH_3)_4(PPh_3)_2$	2.449(2)	2.479(4)	45
$Rh_2(ONHCCF_3)_4(py)_2$	2.472(3)	2.26(1), 2.31(1)	12
$Rh_2(PhCONH)_4(SbPh_3)_2 \cdot CH_2Cl_2$	2.463(1)	2.681(6)	This work
$Rh_2(PhCONH)_4(py)_2$	2.437(1)	2.227(7)	This work
$Rh_2(O_2CCH_3)_4(py)_2$	2.3963(2)	2.227(2)	6

[a]aza = 7-azaindole.

compounds have smaller Rh–Rh distances than amidato compounds. A second steric factor is the size of the axial ligand. Larger repulsive forces between the axial ligand and the coordinated bridging atoms might be expected to stretch the Rh–Rh bond, and this is consistent with the data. Doubtless a complex interplay of both electronic and steric forces is at work and further discussion is not profitable.

Turning now to the electronic spectra of the new compounds (see Table VII), we note that they show considerable variation in detail as a function of solvent and axial ligands. There has been a good deal of experimental and theoretical study of the spectra of the carboxylato bridged compounds [10, 26, 27] culminating in the recent work of Gray and coworkers [53] who have provided convincing evidence for the assignments of the principal absorption bands. While the amidato complexes have spectra that are superficially similar to those of the carboxylates, it would be unjustified to simply assume that comparable assignments are correct. The carboxylates have two dominant absorption bands at *ca.* 400 nm and *ca.* 600 nm which have been assigned [53] to π(Rh–O) → σ^*(Rh–O) and π^*(Rh–Rh) → σ^*(Rh–O) transitions, respectively. Most of the spectra of the amidato compounds also have two main absorptions, falling at <400 nm and $\geqslant 450$ nm. However, since the transitions in the carboxylato molecules strongly involve the Rh–O interactions, and the core symmetry is D_{4h}, whereas for the amidato compounds half the Rh–O bonds are replaced by Rh–N bonds and the symmetry is lowered to only C_{2h}, it is very doubtful that a simply parallel assignment is correct.

Finally, we turn to the electrochemical results. A great deal of attention has already been given to the electron transfer behavior of the dirhodium tetracarboxylato compounds [17, 29, 30, 35, 47–52], from which it is evident that the oxidation potentials (corresponding to loss of a π^* electron from the Rh–Rh bond) are quite sensitive to both the R group in the carboxylate anions and the axial ligands. Work on dirhodium tetraamidate compounds by Bear and coworkers [11–14] has shown a dramatic cathodic shift on changing from RCO_2^- to $RCONR'^-$ ligands, with finer variations caused by changes in the R and R' groups of the $RCONR'^-$ ligands. The results that we have obtained are consistent with those of Bear *et al.*

The frequent appearance of two oxidation processes, one of much larger amplitude than the other, and separated by *ca.* 0.05–0.20 V is presumably due to the presence of a major and a minor species differing in their axial ligands. In several cases coulometric oxidation was carried out at a potential higher than both of these features and it was found that they jointly account for the transfer of one mol of electrons per mol of solute. The oxidation potentials for the $Rh_2(PhCONH)_4$ species lie generally 0.5 to 0.7 V below the range for $Rh_2(CH_3CONH)_4$, which is in accord with the lower basicity of the CF_3CONH^- ligand. This difference can also be viewed from a structural point of view. Since the PhCONH compound has a shorter Rh–Rh bond length, the π^* orbital from which the electron is removed should be less stable.

Acknowledgement

We thank the National Science Foundation for financial support.

Supplementary Material Available

Tables of structure factors, anisotropic thermal parameters and complete list of bond distances and bond angles (41 pages). These are available on request from author F.A.C.

References

1 F. A. Cotton and R. A. Walton, 'Multiple Bonds Between Metal Atoms, Wiley, New York, 1982, chap. 7, p. 311 and refs. therein.
2 T. R. Felthouse, *Prog. Inorg. Chem., 29*, 73 (1982).
3 E. B. Boyer and S. D. Robinson, *Coord. Chem. Rev., 50*, 109 (1983).

4 F. A. Cotton and T. R. Felthouse, *Inorg. Chem., 20*, 600 (1981).
5 F. A. Cotton and T. R. Felthouse, *Inorg. Chem., 20*, 584 (1981).
6 Y. B. Koh and G. G. Cristoph, *Inorg. Chem., 17*, 2590 (1978).
7 M. R. Rhodes and K. R. Mann, *Inorg. Chem., 23*, 2053 (1984).
8 M. Berry, C. D. Garner, I. H. Hillier and W. Clegg, *Inorg. Chim. Acta, 45*, L209 (1980).
9 F. A. Cotton, T. R. Felthouse and S. Klein, *Inorg. Chem., 20*, 3037 (1981).
10 B. E. Bursten and F. A. Cotton, *Inorg. Chem., 20*, 3042 (1981).
11 J. Duncan, T. Malinski, T. P. Zhu, Z. S. Hu, K. M. Kadish and J. L. Bear, *J. Am. Chem. Soc., 104*, 5507 (1982).
12 A. M. Dennis, R. A. Howard, D. Lancon, K. M. Kadish and J. L. Bear, *J. Chem. Soc., Chem. Commun.*, 399 (1982).
13 K. M. Kadish, D. Lancon, A. M. Dennis and J. L. Bear, *Inorg. Chem., 21*, 2987 (1982).
14 T. P. Zhu, M. Q. Ahsan, T. Malinski, K. M. Kadish and J. L. Bear, *Inorg. Chem., 23*, 2 (1984).
15 A. M. Dennis, J. D. Korp, I. Bernal, R. A. Howard and J. L. Bear, *Inorg. Chem., 22*, 1522 (1983).
16 J. D. Korp, I. Bernal and J. L. Bear, *Inorg. Chim. Acta, 51*, 1 (1981).
17 L. A. Bottomley and T. A. Hallberg, *Inorg. Chem., 23*, 1584 (1984).
18 N. Petiniot, A. F. Noels, A. J. Anciaux, A. J. Hubert and Ph. Teyssi, in M. Tsutsui (ed.), 'Fundamental Research in Homogeneous Catalysis', Plenum, New York, 1979, p. 421.
19 N. Petiniot, A. J. Anciaux, A. F. Noels, A. J. Hubert and Ph. Teyssie, *Tetrahedron Lett.*, 1239 (1978).
20 M. Fieser, 'Reagents for Organic Synthesis, Vol. 8', Wiley-Interscience, New York, 1980, p. 434.
21 K. Aoki and H. Yamazaki, *J. Am. Chem. Soc., 106*, 3691 (1984).
22 R. G. Hughes, J. L. Bear and A. P. Kimball, *Proc. Am. Assoc. Cancer Res., 13*, 120 (1972).
23 J. L. Bear, H. B. Gray Jr., L. Rainen, I. M. Chang, R. Howard, G. Serio and A. P. Kimball, *Cancer Chemother. Rep., 59*, 611 (1975).
24 A. Erck, L. Rainen, J. Whileyman, I. Chang, A. P. Kimball and J. L. Bear, *Proc. Soc. Exp. Biol. Med., 145*, 1278 (1974).
25 R. A. Howard, T. G. Spring and J. L. Bear, *Cancer Res., 36*, 4402 (1976).
26 J. G. Norman, Jr. and H. J. Kolari, *J. Am. Chem. Soc., 100*, 791 (1978).
27 J. G. Norman, Jr., A. E. Renzoni and D. A. Case, *J. Am. Chem. Soc., 101*, 5246 (1979).
28 H. Nakatsuji, J. Ushio, K. Kanada, Y. Onishi, T. Kawamura and T. Yonezawa, *Chem. Phys. Lett., 79*, 299 (1981).
29 H. Nakatsuji, Y. Onishi, J. Ushio and T. Yonezawa, *Inorg. Chem., 22*, 1623 (1983).
30 T. Kawamura, K. Fukanachi, T. Sowa, S. Hayashida and T. Yonezawa, *J. Am. Chem. Soc., 103*, 364 (1981).
31 M. Berry, C. D. Garner, I. H. Hillier, A. A. MacDowall and W. Clegg, *J. Chem. Soc., Chem. Commun.*, 494 (1980).
32 C. D. Garner, M. Berry and B. E. Mann, *Inorg. Chem., 23*, 1501 (1984).
33 F. A. Cotton and T. R. Felthouse, *Inorg. Chem., 19*, 323 (1980).
34 F. A. Cotton and T. R. Felthouse, *Inorg. Chem., 19*, 2347 (1980).
35 C. R. Wilson and H. Taube, *Inorg. Chem., 14*, 405 (1975).
36 I. B. Baranovskii, S. S. Abdullaev and R. M. Shchelokov, *Russ. J. Inorg. Chem.*, (Engl. Transl.), *24*, 1753 (1979).
37 L. M. Dikareva, M. A. Porai-Koshits, G. G. Sadikov, I. B. Baranovskii and M. A. Golubnichaya, *Russ. J. Inorg. Chem.* (Engl. Transl.), *23*, 578 (1978).
38 F. A. Cotton, S. Han and W. Wang, *Inorg. Chem., 23*, 4762 (1984).
39 G. A. Rempel, P. Legzdins, H. Smith and G. Wilkinson, *Inorg. Synth., 13*, 90 (1972).
40 A. Bino, F. A. Cotton and P. E. Fanwick, *Inorg. Chem., 18*, 3358 (1979).
41 F. A. Cotton, B. A. Frenz, G. Deganello and A. Shaver, *J. Organomet. Chem., 50*, 227 (1973).
42 A. C. T. North, D. C. Phillips and F. S. Mathews, *Acta Crystallogr., Sect. A:, 24*, 351 (1968).
43 A. R. Chakravarty, F. A. Cotton and D. A. Tocher, *Inorg. Chem.*, in press.
44 A. R. Chakravarty, F. A. Cotton and D. A. Tocher, *J. Am. Chem. Soc., 106*, 6409 (1984).
45 G. G. Christoph and Y. B. Koh, *J. Am. Chem. Soc., 101*, 1422 (1979).
46 F. A. Cotton, B. G. DeBoer, M. D. LaPrade, J. K. Pipal and D. A. Ucko, *Acta Crystallogr., Sect. B:, B27*, 1664 (1971).
47 K. M. Kadish, K. Das, R. A. Howard, A. M. Dennis and J. L. Bear, *Bioelectrochem. Bioenerg., 5*, 741 (1978).
48 R. D. Cannon, D. B. Powell, K. Sarawek and J. S. Stillman, *J. Chem. Soc., Chem. Commun.*, 31 (1976).
49 M. Moszner and J. J. Ziolkowski, *Bull. Acad. Pol. Sci., Ser. Sci. Chim., 24*, 433 (1976).
50 K. Das, K. M. Kadish and J. L. Bear, *Inorg. Chem., 17*, 930 (1978).
51 R. S. Drago, S. P. Tanner, R. M. Richman and J. R. Long, *J. Am. Chem. Soc., 101*, 2897 (1979).
52 T. Sowa, T. Kawamura, T. Shida and T. Yonezawa, *Inorg. Chem., 22*, 56 (1983).
53 V. M. Miskowski, W. P. Schaeffer, B. Sadeghi, B. D. Santarsiero and H. B. Gray, *Inorg. Chem., 23*, 1154 (1984).